Construction of a tree-species classification map using multispectral images of UAVs: A case study of the Dong Rui Commune wetlands, Vietnam

Dung Trung Ngo (ngotrungdung266@gmail.com)
Joint Vietnam-Russia Tropical Science and Technology Research Center

Khanh Quoc Nguyen
Joint Vietnam-Russia Tropical Science and Technology Research Center

Cuong Hung Dang
Joint Vietnam-Russia Tropical Science and Technology Research Center

Ngoc Thi Dang
University of Science, Vietnam National University

Research Article

Keywords: Normalized difference vegetation index, Mangrove, Ecosystem service, Ecosystem management, Visual classification method, Biodiversity assessment

Posted Date: July 7th, 2023

DOI: https://doi.org/10.21203/rs.3.rs-3118278/v1

Abstract

Wetlands provide resources, regulate the environment, and stabilize shorelines; however, they are among the most vulnerable ecosystems in the world. Managing and monitoring wetland ecosystems are important for the development and maintenance of ecosystem services and their sustainable use in the context of climate change. We used Phantom 4 multispectral unmanned aerial vehicles (UAVs) to collect data from wetland areas in the Dong Rui Commune, which is one of the most diverse and valuable wetland ecosystems in northern Vietnam. A tree-species classification map was constructed through a combination of the visual classification method and spectral reflectance values of each plant species, and the characteristic distributions of mangrove plants, including *Bruguiera gymnorrhiza, Rhizophora stylosa*, and *Kandelia obovata*, were determined with an overall accuracy of 91.11% and a kappa coefficient (K) of 0.87. Universal reflectance graphs of each mangrove plant species were constructed for five wave channels, including blue, green, red, red edges, and near-infrared and the normalized difference vegetation index (NDVI). An experiment was conducted to map plant taxonomy in the same area based only on a graph of spectral reflectance values at five single-spectral bands and constructed NDVI values, resulting in an overall accuracy of 78.22% and a K of 0.67. The constructed map is useful for classifying, monitoring, and evaluating the structure of each group of mangroves, thereby enabling the efficient management and conservation of the Dong Rui Commune wetlands.

INTRODUCTION

Wetlands are diverse and rich ecosystems that provide natural resources and have important functions in regulating the environment, providing cultural and tourist services, and many other invaluable benefits. With an area of approximately 7–9 million km^2, accounting for approximately 4–6% of the land surface of the Earth, wetlands are important for human life as they encompass approximately 45% of the natural value provided by ecosystems (Mitsch and Gosselink 2000; Costanza et al. 1997). Mangroves are important habitats for many species of fish and crustaceans, and play an important role in coastal protection and water quality (Vaiphasa 1998). The distribution of plant biomes in mangroves contributes to the maintenance of the stability of wetland ecosystems, reflecting the changes and interactions of natural factors in the region (Peng et al. 2022). Therefore, it is necessary to develop a classification system for plant species in wetland ecosystems for application in resource management, biodiversity assessment, conservation, and ecosystem service development.

Remote sensing can be effectively used for the mapping of forest types based on resource inventory and tree species (Dalponte et al. 2008; Ghosh et al. 2014). Multispectral remote sensing allows for the differentiation of vegetation or other types of objects, such as rocks and soils, clear and turbid water, and selected man-made materials (Govender et al. 2007). In addition, high-resolution remote sensing images allow for the construction of maps with higher accuracies compared to low- and medium-resolution images (Nguyen et al. 2022).

Unmanned aerial vehicles (UAVs) provide ultrahigh-resolution images that are applied in many research disciplines such as geology (Bemis et al. 2014; Lorenz et al. 2017), geomorphology (Autret et al. 2017), meteorology, and hydrology (Bandini et al. 2017). UAVs are increasingly used in forest management, including in the study of biological characteristics of trees such as in the estimation of gaps in forest canopy (Dang Hoi and Trung Dung 2021) and biomass and the classification of plants (Chabot et al. 2018; Eltner et al. 2022). It has become easier and more accurate to collect multispectral UAV images for classifying ground realities within a narrow range using UAV-mounted sensors (Eltner et al. 2022; Honkavaara et al. 2013). A major advantage of using UAV is its high resolution that facilitates a good differentiation between different subjects based on their spectral reflectances in each narrow band (Landgrebe 1999). In addition, because of their low range that minimizes the influence of the atmosphere on the spectral reflectance of each ground object, UAVs are considered suitable tools for narrow-range plant taxonomy (Nevalainen et al. 2017). UAVs can be used to capture images proactively, including during local flooding or low-tide times in wetland ecosystems (Dezhi et al. 2018). However, the use of UAVs in vegetation research has some limitations in adverse weather conditions such as high wind speed and rains owing to their small loads (Nex and Remondino 2014; Matese et al. 2015). Another advantage of UAVs is that it is possible to use 3D data obtained after processing for the determination of the longitudinal structures between species (including tree height, tree type, and canopy distribution) to classify tree species (Tuominen et al. 2018; Näsi et al. 2015). Therefore, UAVs are suitable for small-scale point studies that require proactively receiving data and high accuracy.

Many studies have classified plants based on spectral image data obtained from UAVs. Multispectral imaging data from UAVs were used for the classification of 12 different forest tree species by comparing the spectral reflectances between the visible and near-infrared (NIR) wave bands in a subtropical forest area in southern Brazil (Sothe et al. 2019). In Luozhuang, Changziying town, China, the authors used the blue (466–492 nm), green (494–570 nm), red (642–690 nm), red edge (694–774 nm), and NIR (810–882 nm) bands obtained from cameras installed in UAVs to classify eight overlay objects, including six different tree species (Yunjun et al. 2019). UAVs were used in the classification of seven land-use overlay objects using object-based image analysis (OBIA) in the wetlands of Florida (Liu and Abd-Elrahman 2018). In the Central European forest area, UAVs were used to classify plants based on the reflectance spectrum of each plant species with an accuracy of 78.4%. In India, UAVs have also been used to classify detailed coating types with up to 95% accuracy (Tiwari et al. 2020; Richter et al. 2016). In addition, light detection and ranging (LiDAR) technology, with its ability to provide parameters of height and canopy structure, has also been widely used in forest plant taxonomy (Maltamo et al. 2004, Andersen et al. 2005; Brennan and Webster 2006). In general, the construction of plant taxonomic maps based on remote sensing images is based on the classification of the object and the characteristics of the reflectance spectrum of each plant species.

We focused on classifying many mangrove plants in the wetland area of the Dong Rui Commune, Tien Yen district, Quang Ninh province, Vietnam, based on the multispectral image dataset obtained from Phantom 4 multispectral UAVs combined with the real-time kinematic (RTK) locator. In areas where UAVs are used, the diversity of mangrove plant species is relatively low when only three plant species are identified. However, these species are alternately distributed, forming species combinations, making it difficult to determine their distribution and areas of coverage using conventional field measurement methods. Therefore, high-resolution hyperspectral data with single-wave channel bands, including the blue, green, red, red edge, and NIR bands were used to distinguish individual mangrove species. The main objective of this study was to classify each mangrove plant species using the OBIA method and build a spectral reflectance graph for some mangrove plant species. Results provide a basis for expanding research to build a spectral reflectance graph for many species of mangrove plants in northern Vietnam. The dataset on the spectral reflectance of each plant species will be used for mapping, monitoring, classifying, and managing wetland ecosystems in the Dong Rui Commune wetland area and in other similar areas.

MATERIALS AND METHODS

Study area

The Dong Rui Commune wetland covers an area of 4,902 ha, with geographical coordinates from 21°11 N to 21°33 N and from 107° 13' E to 107° 32' E (People's Committee of Tien Yen district 2015; Fig. 1). This is a coastal accretion region with low terrain that progressively moves to the sea with elevations ranging from 1.5 to 3 meters. Many areas of the marsh have been transformed into arable fields and aquaculture lagoons, while the rest are tidal-flooded beaches and coastal dunes. In the study region, saline soils predominate, whereas alluvial soils are found in the center area, where the local population is concentrated (Ngo et al. 2023).

Mangroves are prevalent in estuary biomes, where they adapt to unpredictable environmental circumstances and are impacted by low and high tides. Because of the physical conditions in the narrow estuary marshes that run down the riverside, groupings of trees are dispersed and create strips (Ngo et al. 2023). Characteristic plant biomes include *Aegiceras corniculatum* superior plant biomes with the plant associations of *Aegiceras corniculatum, Kandelia obovata*, *Bruguiera gymnorhiza*, and *Rhizophora stylosa*, *Aegiceras corniculatum* and *Kandelia obovata*, and *Kandelia obovata*, *Bruguiera gymnorhiza*, and *Rhizophora stylosa* (Huan 2021).

Data collection using UAVs

This study used DJI Phantom 4 multispectral UAVs with six cameras that provide a multispectral imaging system, including one red, green, and blue (RGB) camera and a multispectral camera array with five cameras including the bands blue (Rb): 450 nm ± 16 nm, green (Rg): 560 ± 16 nm, red (Rr): 650 ± 16 nm, red edge (Rre): 730 nm ± 16 nm, and near-infrared (Rnir): 840 ± 26 nm, and all of these at 2 MP with a global shutter on a 3-axis stable gimbal stabilizer. In addition, combining the use of the RTK positioner allows positioning data to be fixed to the center of the complementary metal-oxide semiconductor (CMOS), and ensures that each image uses the most accurate metadata (Fig. 2).

We built a flight route for the UAV using DJI GPS Pro software on an IOS operating system (Fig. 3) using the following flight parameters:

Flight altitude: 60 m above the take-off point.

Image coverage: 80% (horizontal) × 70% (vertical).

Flight conditions: From 7:00 to 8:00 LST during the lowest tide of the day, when the light was low.

Flight date: July 15, 2022.

Postflight image processing of UAVs

The procedure for the postflight UAV-image processing is presented in Fig. 4. In addition to the five maps of single-spectrum wave channels, blue, green, red, red edge, and NIR, the additional the normalized difference vegetation index (NDVI) maps based on UAV imagery were combined.

Normalized difference vegetation index: NDVI is an important indicator in the study of the ecology, growth, development, and fluctuations in food coverage. In addition, this indicator also contributes to warnings regarding crop disease status and crop yield when combined with other indicators. NDVI is widely used in agriculture and forestry. In particular, the application of NDVI aims at detecting area fluctuations between different periods within a fixed range. In addition, the index contributes to the assessment of crop development and forecasting yields through the application of UAVs in the agricultural sector.

The NDVI was calculated as follows (Rouse et al. 1974; Tucker 1979):

$$\mathrm{NDVI} = \frac{\mathrm{R_{nir}} - \mathrm{R_r}}{\mathrm{R_{nir}} + \mathrm{R_r}} \quad (1)$$

With: R_{nir}: near-infrared band (840 ± 26 nm); R_r: red band (650 ± 16 nm)

Field data

The area covered by the UAVs was divided into two zones designated as UAVs-01 and UAVs-02. The UAVs-01 area is the space for mapping the classification of tree species based on a combination of image classification methods and spectral reflectance characteristics of each plant species. The UAVs-02 area is the mapping area that verifies the accuracy of the spectral reflectance graph set for each plant species.

Field surveys were conducted in the area covered by the UAVs along route points for the construction of an interpretive image lock for the process of mapping and evaluating the accuracy of the map for UAVs-01 (1,516 image lock points). Of these, 75% of the lock points were used to interpret and map mangrove plant taxonomy, and the remaining 25% (corresponding to 379 image lock points) were used to assess map accuracy (Fig. 5). Species identification was conducted in the field due to the low diversity of mangrove plant species in the flying zone of UAVs.

Construction of a spectral reflectance graph and a tree-species classification map

Validation of classification results

Ecognition software was used to classify and interpret images based on key patterns of image decoding using the object-oriented classification method (Nussbaum and Menz 2008). Each species of mangrove plants was recorded and classified according to its characteristics, such as image tone, structure, shape, and relationship to neighboring regions. In addition, the reflectance values of each plant species was recorded for five single-spectrum wave channels, including the blue, green, red, red edge, and NIR bands, and NDVI values were calculated based on multispectral image processing (Fig. 6). This is a supervised classification method that is based on the principle of the difference in reflectance between coating objects.

A random selection approach with at least 10 points for each state was employed to examine the outcomes of picture interpretation, followed by verification of the present status in the field and comparison with interpreted findings. If the accuracy is less than 75%, the interpreter must reassess the decoding procedure and technique of getting the decryption key in order to increase the map's accuracy after categorization. This procedure requires the following steps.

An error matrix (confusion matrix) was formed between the classification results and the control sample, and the kappa coefficient (K) was calculated. Kappa was first introduced in 1960 by Cohen as a reliability statistic when two judges classified targets into categories for a nominal variable (Cohen 1960). K assesses the reliability of maps based on preliminary and fact-checked results, and it has been used in many studies of remote sensing-based mapping (Nguyen et al. 2022; Pardo-Iguzquiza et al. 2018).

K is the utility factor of all primes from the error matrix and was employed as a measure of classification accuracy. Rows and columns represent the basic difference between actual values and the matrix's deviation error, as well as the overall number of changes (McGrath 2010), https://doi.org/10.1002/9780470479216.corpsy0484. The formula for calculating K is as follows:

$$K = \frac{N\sum_{i=1}^{r} X_{ii} - \sum_{i=1}^{r}(X_{i+} - X_{+i})}{N^2 - \sum_{i=1}^{r}(X_{i+} - X_{+i})} (2)$$

where r is the number of columns in the image matrix, and X_{ii} denotes the number of pixels seen in row i and column i (on the main diagonal). The total number of pixels seen in row i is given by X_{i+}, and the total number of pixels observed in the image matrix is given by N. K is typically between 0 and 1, with values in this range indicating adequate classification accuracy. According to the US Geological Survey, K values are divided into three categories: K 0.8 indicates great precision; K 0.4 indicates moderate accuracy; and K 0.4 indicates poor accuracy (Nguyen et al. 2022).

Random forest algorithm

A random forest algorithm was used to enhance the accuracy of mangrove plant taxonomy maps in the Dong Rui Commune. Breiman (2001) proposed the random forest algorithm, which allows the classification of forest trees based on the regression method. The random forest algorithm includes two additional pieces of information such as a measure of the importance of the predictor variables and a measure of the internal structure of data (the proximity of different data points to one another). The random forest algorithm is widely used in classification, forest inventory mapping, and forest tree classification with enhanced accuracy of different types of thematic maps (Francke et al. 2008; Prinzie and Van den Poel 2007).

Estimation of accuracy of plant taxonomy maps based on spectral reflectance graphs

After constructing a set of spectral reflectance graphs for each plant species for the five monochromatic spectral bands and NDVI values, the classification of mangrove coverage by plant species was carried out based solely on the newly constructed spectral reflectance graph in the UAVs-02 area. The UAVs-02 area is on the same route as that of the UAVs-01 area, and hence, has similar weather conditions, ceilings, and flight parameters of UAVs. After constructing the mangrove vegetation classification map for point UAVs-02, we performed accuracy assessment at 179 field survey sites (Fig. 7) by calculating the overall accuracy and K.

RESULTS

Construction of a spectral reflectance graph set

Based on the photo lock points and the results of the classification of each mangrove plant species at UAVs-01, spectral reflectance graphs for the three mangrove plant species were developed for five monochromatic spectral bands with NDVI values of each species (Figs. 8–11).

The spectral reflectance values for *Bruguiera gymnorrhiza* were 4–14, 5–22, 1–2 in the blue, green, and red bands, respectively (Fig. 8). The spectral reflectance values of the red edge and NIR bands fluctuate greatly, especially in the NIR band (25–90). The mean spectral reflectance value was the highest for the red-edge band at 60 (Fig. 8). NDVI values were highly stable, ranging from 0.8–0.9.

The spectral reflectance values for *Rhizophora stylosa* in the blue and green bands were 3–30 (Fig. 9), and for the red band they were relatively uniform at 1–5. The spectral reflectance values fluctuate widely in the red edge and NIR bands, especially in the red edge band ranging from 20 to 135. For the NIR band, the spectral reflectance values ranged from 20 to 110, averaging 60. NDVI values were highly stable at 0.8–0.9 (Fig. 9).

For *Kandelia obovata*, the shape of the lines expressing the reflectance spectral value was quite similar to that of *Rhizophora stylosa*. According to Fig. 10, in the blue and green bands, the spectral reflectance value ranged between 3 and 20. In the red band, the spectral reflectance value was relatively uniform, ranging from 1 to 5. For the red-edge band, the spectral reflectance value was the highest compared to the other bands (the average value was 45 and range was 20–100). The spectral reflectance value for the NIR band was 40, ranging from 20 to 85. NDVI values were highly stable at 0.8–0.9 (Fig. 10).

According to Fig. 11, the differences between *Bruguiera gymnorrhiza*, *Rhizophora stylosa*, and *Kandelia obovata* are evident in the blue and green bands, and especially in the red edge and NIR bands. Accordingly, in the red-edge band, the reflectance values of *Rhizophora stylosa* were the highest at approximately 78, followed by *Bruguiera gymnorrhiza* and *Kandelia obovata* with value thresholds of 75 and 62, respectively. Similarly, for the NIR band, the reflectance value of *Rhizophora stylosa* was the highest, followed by *Bruguera gymnorrhiza* and *Kandelia obovata* at 63, 58, and 52, respectively (Fig. 11). In the blue and green bands, the spectral reflectance values of these three mangrove plant species were not significantly different ranging from 5 to 7. No difference was observed between the spectral reflectance values of the three plant species between the red band and NDVI values, and they were relatively low and similar (Fig. 11).

Accuracy assessment of map

The overall accuracy of the map is presented in Table 1. K values were determined based on formula (2). According to Table 1, the overall accuracy of the regional tree-species classification map of UAVs-01 was 91.11%, corresponding to a K of 0.86 (high accuracy). The user accuracy value for *Kandelia obovata* was the highest at 99.16%, and the lowest was for *Bruguiera gymnorrhiza* at 75%. The highest producer accuracy value was obtained for *Bruguiera gymnorrhiza* at 96% and *Kandelia obovata* had the lowest value at 88.06%.

According to Table 1, only 4% of all samples (corresponding to 1/25 of the sample) of *Bruguiera gymnorrhiza* were misinterpreted as *Rhizophora stylosa*. Only 3.6% of all samples belonging to *Rhizophora stylosa* were misinterpreted as *Bruguiera gymnorrhiza*, accounting for eight out of 220 samples. However, 11.9% of all samples of *Kandelia obovata* were misinterpreted as *Rhizophora stylosa*, corresponding to 16 of 134 samples.

Table 1 Confusion matrix of the classification algorithm for the UAVs-01 area

		Ground Reference			**Total**
		Bruguiera gymnorrhiza	*Rhizophora stylosa*	*Kandelia obovata*	
Classification	*Bruguiera gymnorrhiza*	**24**	1		**25**
	Rhizophora stylosa	8	**211**	1	**220**
	Kandelia obovata		16	**118**	**134**
Total		32	228	119	**379**
User Accuracy (%)		75.00	92.54	99.16	**88.90**
Producer Accuracy (%)		96.00	95.91	88.06	**93.32**
Overall Accuracy (%)					**91.11**

Construction of a tree-species classification map

A tree-species classification map was constructed for the distribution of *Bruguiera gymnorrhiza*, *Rhizophora stylosa*, and *Kandelia obovata* in the UAVs-01 area. (Fig. 12). *Kandelia obovata* was highly concentrated in areas close to river flows, where the terrain is lower, and in tidal flat areas. *Rhizophora stylosa* is predominant in the tidal flat areas. *Bruguiera gymnorrhiza* and *Rhizophora stylo*sa are often alternately distributed together, forming plant associations that characterize the UAVs-01 flying area in particular and in the northwest of the Dong Rui Commune in general.

In the UAVs-01 region, *Rhizophora stylosa* was dominant in terms of distribution area with 67% of mangrove coverage for the entire region. *Kandelia obovata* had a total distribution area of 20%, while *Bruguiera gymnorrhiza* had the lowest distribution area at 13%. Structurally, *Kandelia obovata* populations have a low height of 1–1.5 m and have a small canopy. The plant association consisted of *Bruguiera gymnorrhiza* and *Rhizophora stylosa* with a height of 3–4 m and a wide canopy.

Verification of the accuracy of spectral reflectance graphs

Based on the spectral reflectance values of *Bruguiera gymnorrhiza, Rhizophora stylosa*, and *Kandelia obovata* in the UAVs-01 area, a tree-species classification map for the UAVs-02 area was constructed (Fig. 13). In the UAVs-02 area, similar to the UAVs-01 area, *Kandelia obovata* is highly concentrated in areas close to river flows, where the terrain is lower, and in tidal flat areas. The plant association consists of *Bruguiera gymnorrhiza* and *Rhizophora stylosa*, which are often alternately distributed in tidal flat areas with the latter dominating.

In the UAVs-02 region, *Rhizophora stylosa* was dominant in terms of distribution area, accounting for 63% of the total mangrove coverage of the entire region. *Kandelia obovata* and *Bruguiera gymnorrhiza* had similar distribution areas of 19 and 18%, respectively. Accuracy assessment of the tree-species classification map was performed based on 179 field survey sites in the UAVs-02 area (Table 2).

Table 2 Confusion matrix of classification algorithm for the UAVs-02 area

		Ground Reference			Total
		Bruguiera gymnorrhiza	*Rhizophora stylosa*	*Kandelia obovata*	
Classification	*Bruguiera gymnorrhiza*	**22**	7		**29**
	Rhizophora stylosa	9	**86**	2	**97**
	Kandelia obovata	1	18	**34**	**53**
Total		32	111	36	**179**
User Accuracy (%)		68.75	77.48	94.44	**80.22**
Producer Accuracy (%)		75.86	88.66	64.15	**76.22**
Overall Accuracy (%)					**78.22**

According to Table 2, the overall accuracy of the tree-species classification map of UAVs-02 is 78.22%, corresponding to a K of 0.67 (moderate accuracy). *Kandelia obovata* had the highest user accuracy value of 94.44% and *Bruguiera gymnorrhiza* had the lowest of 68.75%. The highest producer accuracy value was observed for *Rhizophora stylosa* (88.66%) and the lowest for *Kandelia obovata* (64.15%). 24% of all samples (7/29) of *Bruguiera gymnorrhiza* were misinterpreted as *Rhizophora stylosa*. 9.2% of all R*hizophora stylosa* samples were misinterpreted as *Bruguiera gymnorrhiza*, corresponding to 9 out of 97 samples. Of the 34 *Kandelia obovata* samples 18 were misjudged as *Rhizophora stylosa*, accounting for 52.9%.

DISCUSSION

Despite their importance, wetlands remain among the most vulnerable ecosystems on Earth (Millennium Ecosystem Assessment 2005). Wetlands are being lost at a faster rate than any other ecosystem with more than half of them being degraded or lost in the past 150 years (Sica et al. 2016; Slager et al. 2019). Therefore, measures should be taken to restore this most important ecosystem, including strengthening management and monitoring based on technological applications (Baranyai and Benkô 2012). Classification of mangrove vegetation, which determines the level of biodiversity of this ecosystem, is the basis for management, monitoring, and conservation measures (Pellegrini et al. 2009). UAV images with a high resolution are essential for ecological research in narrow spaces. We prepared tree-species classification maps using images from UAVs mounted with multispectral cameras in the wetland area of the Dong Rui Commune. Results identified three mangrove plant species, thereby enabling the construction of a library of spectral reflectances for each plant species with respect to five monochromatic wave bands (green, blue, red, red edge, and NIR) and their NDVI value sets. Unlike UAVs with only RGB wave bands that allow the identification of only some simple indicators, such as gaps in forest canopy in the Dong Rui mangrove forest (Hanh et al. 2018), the UAVs used by us are capable of capturing multispectral images and identifying plant indicators and spectral reflectance values of different spectral wave bands. The images obtained from the UAVs were capable of identifying up to 21 different plant indices based on data of five single-spectral wave bands (Hunt et al. 2013). In addition, in addition to the ability to actively capture ultrahigh-resolution images, UAVs are also capable of accurately determining the structure of mangrove vegetation, such as tree height and coverage (Gupta et al. 2018).

Combining visual classification with characteristic reflectance spectral values of each plant species resulted in a more accurate map than that obtained through classification based on reflectance spectral values alone (overall accuracy was 91.11 and 78.22%, respectively). The most effective spectral range was between 393 and 700 nm for the determination of tree taxonomy (Peerbhay et al. 2014), corresponding to the four spectral bands of Phantom 4 UAVs, including red, green, blue, and red edge. In particular, the greatest differences in each plant species in the Dong Rui Commune area are in the green, red edge, and NIR spectra, and this is similar to studies of the reflectance spectra of plants in the Central European area (Fassnacht et al. 2014). Wavebands with values ranging from 393 to 723 nm show the best ability to distinguish between plants (Peerbhay et al. 2013). However, the map provided lower accuracy when using only the spectral reflectance of individual mangrove plants compared to results obtained by incorporating additional imaging classification methods. In the Dong Rui Commune wetland area, the mangrove plant biome consists of *Bruguiera gymnorrhiza* and *Rhizophora stylosa*, which often grow alternately, resulting in the canopy of these species being mixed together. The distinction between the two species in the field was mainly based on their morphologies, with differences in leaf shape, fruit, stem structure, and roots. This is a limitation of images obtained from the UAVs, as the roots of the mangrove vegetation in the image were obscured by the trees.

The diversity of mangrove species in the Dong Rui Commune is relatively wide compared with the mangrove areas of northern Vietnam, such as the Cat Ba and Phu Long–Gia Luan regions, and the Hai Phong Province (Thinh et al. 2008; Pham et al. 2017). The wetland ecosystem is considered to be the most diverse in northern Vietnam compared with that of the Xuan Thuy National Park (Nam Dinh Province). The level of biodiversity of the Dong Rui Commune mangrove forest area is approximately 1,500 species (Huan 2021; Nhan et al. 2015).

The height of the mangrove plant biomes in the Dong Rui Commune wetland area was relatively less. In the tidal flat area, *Bruguiera gymnorrhiza* and *Rhizophora stylosa* had an average height of only 4–5 m. Compared to mangrove areas in southern Vietnam, such as U Minh Ha National Park (the height of *Melaleuca alternifolia* is 10–12 m; Safford et al. 1998) or Tram Chim National Park (Viet et al. 2020), this height is a much lower. This difference is probably because of the thinner mud and sand substrate sediments in the northern region compared to those in the southern region (Huan 2021). In addition, northern Vietnam is subject to many impacts from typhoons (average 5.2 storms per year) (Toan 2014), and hence, mangrove flora cannot have better heights (People's Committee of Tien Yen district 2015; Van et al. 2022).

CONCLUSIONS

In this study, based on multispectral image data obtained using UAVs, spectral reflectance graphs of three plant species and a tree-species classification map were developed for the Dong Rui Commune wetland area. We propose that UAVs are effective tools for obtaining highly accurate plant taxonomy in small-scale areas. Combining the visual classification method and the use of spectral reflectance graphs of plant species enhances the accuracy of classification of tree species maps. However, UAVs are limited by their small scale of coverage of approximately 200 hectares. Therefore, mapping of large-scale areas combining high-resolution satellite imagery and “key lock points” of UAV can be highly beneficial for preparing detailed tree-species maps of small areas. Results of this study can provide the basis for managers to develop options for monitoring fluctuations, and managing and conserving wetland ecosystems in a timely and effective manner. Further technological development of UAVs in terms of improvements in flight time, speed, and weather resistance will enable them to be effective support tools for researchers and managers to monitor and conserve wetland ecosystems.

Declarations

Author contributions: To complete the article, the authors participated in different stage of the study with the following contents: “Dung Trung Ngo and Ngoc Thi Dang conceived and designed the article; Dung Trung Ngo and Khanh Quoc Nguyen wrote the draft; Dung Trung Ngo and Cuong Hung Dang analyzed the data; Cuong Hung Dang controlled UAV in field survey; Dung Trung Ngo drafted the final paper**.”**

Acknowledgements: This work was performed with the support of the project "Application of remote sensing technology and unmanned aerial vehicle to assess the change of wetland ecosystems" chaired by the Institute of Tropical Ecology, Joint Vietnam-Russia Tropical Science and Technology Research Center.

Funding: No funds, grants, or other support was received.

Competing Interests: The authors declare that they have no conflict of interest.

Data statement: All data generated or analysed during this study are included in this published article

References

1. Andersen H-E, McGaughey R and Reutebuch S (2005) Estimating forest canopy fuel parameters using LIDAR data. Remote Sensing of Environment:441-449. doi: https://doi.org/10.1016/j.rse.2004.10.013
2. Autret R, Dodet G, Suanez S, Roudaut G and Fichaut B (2017) Long–term variability of supratidal coastal boulder activation in Brittany (France). Geomorphology. doi: https://doi.org/10.1016/j.geomorph.2017.12.028
3. Bandini F, Butts M, Jacobsen T and Bauer-Gottwein P (2017) Water level observations from Unmanned Aerial Vehicles for improving estimates of surface water-groundwater interaction. Hydrological Processes. doi: https://doi.org/10.1002/hyp.11366
4. Baranyai A and Benkô D (2012) Wetlands: Ecology, management and conservation.
5. Bemis S, Micklethwaite S, Turner D, James M, Akciz S, Thiele S and Bangash H (2014) Ground-based and UAV-Based photogrammetry: A multi-scale, high-resolution mapping tool for Structural Geology and Paleoseismology. Journal of Structural Geology. doi: https://doi.org/10.1016/j.jsg.2014.10.007

6. Breiman L. (2001) Random forests. Machine Learning:5–32.
7. Brennan R and Webster T (2006) Object-oriented land cover classification of LIDAR-derived surfaces. Canadian Journal of Remote Sensing. doi: https://doi.org/10.5589/m06-015
8. Cao J, Leng W, Liu K, Liu L, he Z and Zhu Y (2018) Object-Based Mangrove Species Classification Using Unmanned Aerial Vehicle Hyperspectral Images and Digital Surface Models. Remote Sensing:89. doi: 10.3390/rs10010089
9. Chabot D, Dillon C, Shemrock A, Weissflog N and Sager E (2018) An Object-Based Image Analysis Workflow for Monitoring Shallow-Water Aquatic Vegetation in Multispectral Drone Imagery. International Journal of Geo-Information:294. doi: https://doi.org/10.3390/ijgi7080294
10. Cohen J (1960) A Coefficient of Agreement for Nominal Scales. Educational and Psychological Measurement:37-46. doi: https://doi.org/10.1177/001316446002000104?journalCode=epma
11. Costanza R, Arge, Groot R, Farberk S, Grasso M, Hannon B, Limburg K, Naeem S, neill R, Paruelo J, Raskin R, Sutton P and Belt M (1997) The Value of the World's Ecosystem Services and Natural Capital. Nature:253-260. doi: https://doi.org/10.1016/S0921-8009(98)00020-2
12. Dalponte M, Bruzzone L and Gianelle D (2008) Fusion of Hyperspectral and LIDAR Remote Sensing Data for Classification of Complex Forest Areas. Geoscience and Remote Sensing, IEEE Transactions on:1416-1427. doi: https://doi.org/10.1109/TGRS.2008.916480
13. Dang Hoi N and Trung Dung N (2021) Seasonal Dynamics of Tropical Forest Vegetation in Ngoc Linh Nature Reserve, Vietnam Based on UAV Data. Forest and Society:376-389. doi: https://doi.org/10.24259/fs.v5i2.13027
14. Dezhi W, Wan B, Qiu P, Su Y, Guo Q, Wang R, Sun F and Wu X (2018) Evaluating the Performance of Sentinel-2, Landsat 8 and Pléiades-1 in Mapping Mangrove Extent and Species. Remote Sensing:1468. doi: https://doi.org/10.3390/rs10091468
15. Eltner A, Hoffmeister D, Kaiser A, Karrasch P, Klingbeil L, Stöcker C and Rovere A (2022) UAVs for the Environmental Sciences.
16. Fassnacht F, Neumann C, Förster M, Buddenbaum H, Ghosh A, Clasen A, Joshi P and Koch B (2014) Comparison of Feature Reduction Algorithms for Classifying Tree Species With Hyperspectral Data on Three Central European Test Sites. IEEE Journal of Selected Topics in Applied Earth Observations and Remote Sensing:2547-2561. doi: https://doi.org/10.1109/JSTARS.2014.2329390
17. Francke T, López-Tarazón JA and Schröder B (2008) Estimation of suspended sediment concentration and yield using linear models, Random Forests and Quantile Regression Forests. Hydrological Processes:4892-4904. doi: https://doi.org/10.1002/hyp.7110
18. Ghosh A, Fassnacht F, Joshi PK and Koch B (2014) A framework for mapping tree species combining hyperspectral and LiDAR data: Role of selected classifiers and sensor across three spatial scales. International Journal of Applied Earth Observation and Geoinformation:49–63. doi: https://doi.org/10.1016/j.jag.2013.05.017
19. Govender M, Chetty K and Bulcock H (2007) A review of hyperspectral remote sensing and its application in vegetation and water resource studies. Water SA. doi:

https://doi.org/10.4314/wsa.v33i2.49049

20. Gupta S, Syed M, Hasan M, Faroque M, Jannat M, Munira S and Meem M (2018) Potentials of Unmanned Aerial Vehicle (UAV) in Mangrove Forest Management.
21. Hanh N, Tuan M, Pham T and Hanh N (2018) Characteristics of gap regeneration in mangrove forests of Dong Rui, Tien Yen, Quang Ninh. Biological of Journal. doi: https://doi.org/10.15625/0866-7160/v40n2.13243
22. Honkavaara E, Saari H, Kaivosoja J, Pölönen I, Hakala T, Litkey P, Mäkynen J and Pesonen L (2013) Processing and Assessment of Spectrometric, Stereoscopic Imagery Collected Using a Lightweight UAV Spectral Camera for Precision Agriculture. Remote Sensing:5006-5039. doi: https://doi.org/10.3390/rs5105006
23. Huan NC (2021) Established Dong Rui Wetland Reserve, Tien Yen, Quang Ninh Province. Department of Natural Resources and Environment of Quang Ninh province, Quang Ninh, pp 348
24. Hunt ERJ, Doraiswamy C, McMurtrey J, Daughtry C, Perry E and Akhmedov B (2013) A visible band index for remote sensing leaf Chlorophyll content at the Canopy Scale. International Journal of Applied Earth Observation and Geoinformation:103–112. doi: https://doi.org/10.1016/j.jag.2012.07.020
25. Jiang Y, Zhang L, Yan M, Qi J, Fu T, Fan S and Chen B (2021) High-Resolution Mangrove Forests Classification with Machine Learning Using Worldview and UAV Hyperspectral Data. Remote Sensing:1529. doi: 10.3390/rs13081529
26. Landgrebe D (1999) Some fundamentals and methods for hyperspectral image data analysis. Proceedings of SPIE - The International Society for Optical Engineering. doi: https://doi.org/10.1117/12.346731
27. Liu T and Abd-Elrahman A (2018) Multi-view object-based classification of wetland land covers using unmanned aircraft system images. Remote Sensing of Environment. doi: https://doi.org/10.1016/j.rse.2018.06.043
28. Lorenz S, Zimmermann R and Gloaguen R (2017) The Need for Accurate Geometric and Radiometric Corrections of Drone-Borne Hyperspectral Data for Mineral Exploration: MEPHySTo—A Toolbox for Pre-Processing Drone-Borne Hyperspectral Data. Remote Sensing. doi: https://doi.org/10.3390/rs9010088
29. Maltamo M, Eerikäinen K, Pitkänen J, Hyyppä J and Vehmas M (2004) Estimation of timber volume and stem density based on scanning laser altimetry and expected tree size distribution functions. Remote Sensing of Environment:319-330. doi: https://doi.org/10.1016/j.rse.2004.01.006
30. Matese A, Toscano P, Di Gennaro S, Genesio L, Vaccari F, Primicerio J, Claudio B, Zaldei A, Bianconi R and Gioli B (2015) Intercomparison of UAV, Aircraft and Satellite Remote Sensing Platforms for Precision Viticulture. Remote Sensing:2971-2990. doi: https://doi.org/10.3390/rs70302971
31. McGrath R, Kappa coefficient, in: The Corsini Encyclopedia of Psychology, 2010, https://doi.org/10.1002/9780470479216.corpsy0484
32. Millennium Ecosystem Assessment (2005) Ecosystems and human well-being: wetlands and water.

33. Mitsch W and Gosselink J (2000) The Value of Wetlands: Importance of Scale and Landscape Setting. Ecological Economics:25-33. doi: https://doi.org/10.1016/S0921-8009(00)00165-8
34. Näsi R, Honkavaara E, Paivi L-S, Blomqvist M, Litkey P, Hakala T, Viljanen N, Tuula K, Tanhuanpää T and Holopainen M (2015) Using UAV-Based Photogrammetry and Hyperspectral Imaging for Mapping Bark Beetle Damage at Tree-Level. Remote Sensing:15467-15493. doi: https://doi.org/10.3390/rs71115467
35. Nevalainen O, Honkavaara E, Tuominen S, Viljanen N, Hakala T, Yu X, Hyyppä J, Saari H, Pölönen I, Imai N and Tommaselli A (2017) Individual Tree Detection and Classification with UAV-Based Photogrammetric Point Clouds and Hyperspectral Imaging. Remote Sensing:185. doi: https://doi.org/10.3390/rs9030185
36. Nex F and Remondino F (2014) UAV for 3D mapping applications: A review. Applied Geomatics. doi: https://doi.org/10.1007/s12518-013-0120-x
37. Ngo, D. T., Nguyen, H. D., & Nguyen, H. C. (2023). Assessment of fluctuations in wetland ecosystem areas resulting from anthropogenic activities in the Dong Rui commune, Quang Ninh Province, Vietnam. Heliyon, 9(6), e16984. doi: https://doi.org/10.1016/j.heliyon.2023.e16984
38. Nguyen DH, Ngo TD, Vu VD and Du QVV (2022) Establishing distribution maps and structural analysis of seagrass communities based on high-resolution remote sensing images and field surveys: a case study at Nam Yet Island, Truong Sa Archipelago, Vietnam. Landscape and Ecological Engineering. doi: https://doi.org/10.1007/s11355-022-00502-0
39. Nhan HTT, Hai HT and Canh LX (2015) Biological deversity in Xuan Thuy National Park, Nam Dinh Province. The 5th National Scientific Conference on Ecology and Biological Resources. Ha Noi, pp 587 - 594
40. Nussbaum S and Menz G (2008) eCognition Image Analysis Software. pp 29-39
41. Pardo-Iguzquiza E, Dowd P, Ruiz-Constán A, Martos-Rosillo S, Luque-Espinar JA, Rodriguez-Galiano V and Pedrera A (2018) Epikarst mapping by remote sensing. Catena:1-11. doi: https://doi.org/10.1016/j.catena.2018.01.026
42. Peerbhay K, Mutanga O and Ismail R (2013) Commercial tree species discrimination using airborne AISA Eagle hyperspectral imagery and partial least squares discriminant analysis (PLS-DA) in KwaZulu–Natal, South Africa. ISPRS Journal of Photogrammetry and Remote Sensing:19–28. doi: https://doi.org/10.1016/j.isprsjprs.2013.01.013
43. Peerbhay K, Mutanga O and Ismail R (2014) Does simultaneous variable selection and dimension reduction improve the classification of Pinus forest species? Journal of Applied Remote Sensing:085194-085194. doi: https://doi.org/10.1117/1.JRS.8.085194
44. Pellegrini J, Soares M, Chaves F, Estrada G and Cavalcanti V (2009) A Method for the Classification of Mangrove Forests and Sensitivity/ Vulnerability Analysis. Journal of Coastal Research:443-447.
45. Peng T, Cao L, Li J, Pu R, Liu Y, Zhang H and Wang C (2022) Ecosystem Stability Assessment of Yancheng Coastal Wetlands, a World Natural Heritage Site. Land:564. doi: https://doi.org/10.3390/land11040564

46. People's Committee of Tien Yen district (2015) General report on socio-economic development master plan of Tien Yen district to 2020, orientation to 2030. Quang Ninh,
47. Pham TD, Yoshino K and Kaida N (2017) Monitoring Mangrove Forest changes in Cat Ba Biosphere Reserve using ALOS PALSAR Imagery and a GIS-based Support Vector Machine Algorithm. International Conference on Geo-Spatial Technologies and Earth Resource. Springer International Publishing, pp 103-118
48. Prinzie A and Van den Poel D (2007) Random Multiclass Classification: Generalizing Random Forests to Random MNL and Random NB.
49. Richter R, Reu B, Wirth C, Doktor D and Vohland M (2016) The use of airborne hyperspectral data for tree species classification in a species-rich Central European forest area. International Journal of Applied Earth Observation and Geoinformation:464-474. doi: https://doi.org/10.1016/j.jag.2016.07.018
50. Rouse J, Haas R, Schell J and Deering D (1974) Monitoring Vegetation Systems in the Great Plains with ERTS. NASA Special Publication.
51. Safford RJ, Tran T, Maltby E and Ni D (1998) Status, biodiversity and management of the U Minh wetlands, Vietnam. Tropical Biodiversity:217-244.
52. Sica Y, Quintana R, Radeloff V and Gavier-Pizarro G (2016) Wetland loss due to land use change in the Lower Paraná River Delta, Argentina. Science of The Total Environment. doi: https://doi.org/10.1016/j.scitotenv.2016.04.200
53. Slager B, Tsendbazar N-E, Vollrath A and Reiche J (2019) Mapping wetland characteristics using temporally dense Sentinel-1 and Sentinel-2 data: A case study in the St. Lucia wetlands, South Africa. International Journal of Applied Earth Observation and Geoinformation:102009. doi: https://doi.org/10.1016/j.jag.2019.102009
54. Sothe C, Dalponte M, Almeida d, Schimalski M, Lima, Liesenberg V, Miyoshi G and Tommaselli A (2019) Tree Species Classification in a Highly Diverse Subtropical Forest Integrating UAV-Based Photogrammetric Point Cloud and Hyperspectral Data. Remote Sensing:1338. doi: https://doi.org/10.3390/rs11111338
55. Thinh N, Huan N, Pham U and Sơn Tùng N (2008) Landscape ecological planning based on change analysis: A case study of mangrove restoration in Phu Long-Gia Luan area, Cat Ba Archipelago. VNU Journal of Science, Earth Sciences 133-144.
56. Tiwari A, Sharma S, Dixit A and Mishra V (2020) UAV Remote Sensing for Campus Monitoring: A Comparative Evaluation of Nearest Neighbor and Rule-Based Classification. Journal of the Indian Society of Remote Sensing. doi: https://doi.org/10.1007/s12524-020-01268-4
57. Toan D (2014) Statistical assessment of the properties of the East Sea and the coast of Vietnam in the period 1951-2013. Estuarine and Coastal Marine Science:13.
58. Tucker C (1979) Red and Photographic Infrared Linear Combinations for Monitoring Vegetation. Remote Sensing of Environment. doi: https://doi.org/10.1016/0034-4257(79)90013-0

59. Tuominen S, Näsi R, Honkavaara E, Balazs A, Hakala T, Viljanen N, Pölönen I, Saari H and Ojanen H (2018) Assessment of Classifiers and Remote Sensing Features of Hyperspectral Imagery and Stereo-Photogrammetric Point Clouds for Recognition of Tree Species in a Forest Area of High Species Diversity. Remote Sensing:714. doi: https://doi.org/10.3390/rs10050714
60. Vaiphasa C (1998) Remote sensing techniques for mangrove mapping.
61. Van T, Nguyen Dang M, Khiem M, Duong TH, Van K, Thanh T, Quoc T and Minh T (2022) Climatic Factors Associated with Heavy Rainfall in Northern Vietnam in Boreal Spring. Advances in Meteorology:1-14. doi: https://doi.org/10.1155/2022/5917729
62. Viet H, Potokin A, Anh D, Nguyen T and Nguyen T (2020) Forest Vegetation Cover in Tram Chim National Park in Southern Vietnam. IOP Conference Series: Earth and Environmental Science:012014. doi: https://doi.org/10.1088/1755-1315/574/1/012014
63. Yunjun Y, Deng H, Liu Y and Zhu (2019) Application of UAV-Based Multi-Angle Hyperspectral Remote Sensing in Fine Vegetation Classification. Remote Sensing:2753. doi: https://doi.org/10.3390/rs11232753

Figures

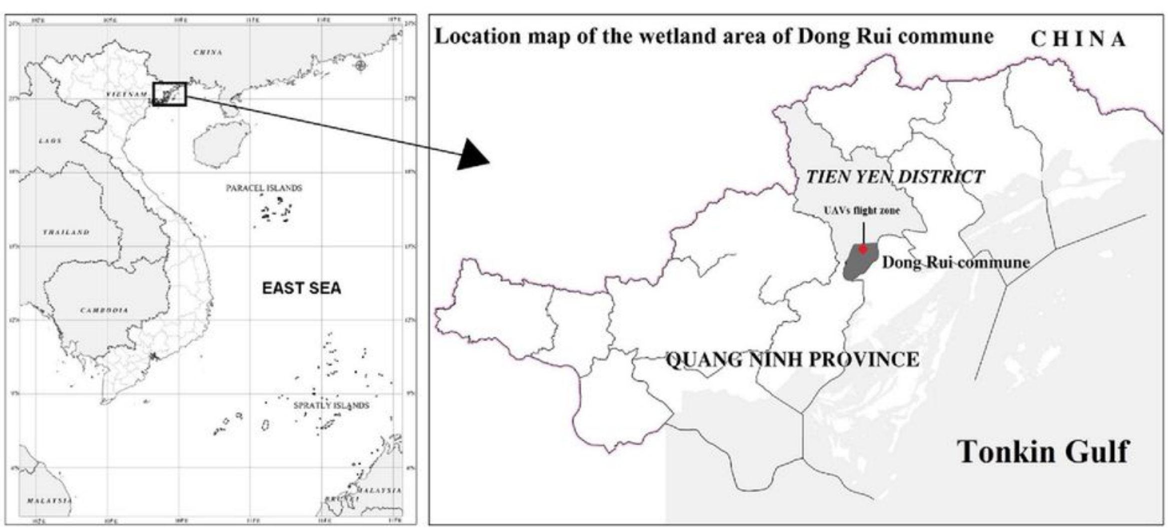

Figure 1

Map of the Dong Rui Commune wetland area

Figure 2

DJI Phantom 4 Multispectral UAV and field deployment with RTK locator

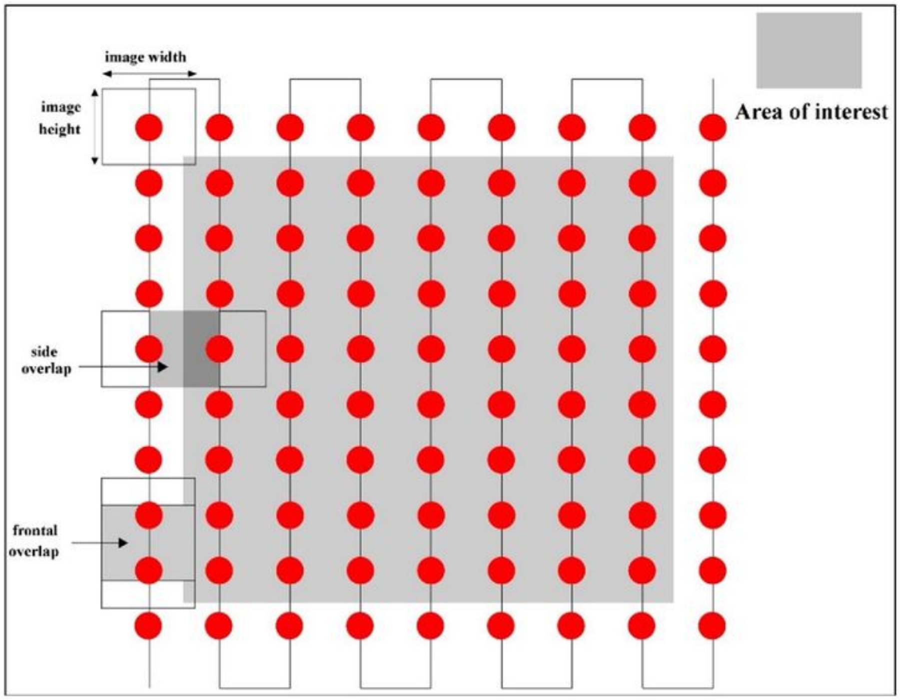

Figure 3

Route designed using DJI GPS Pro software

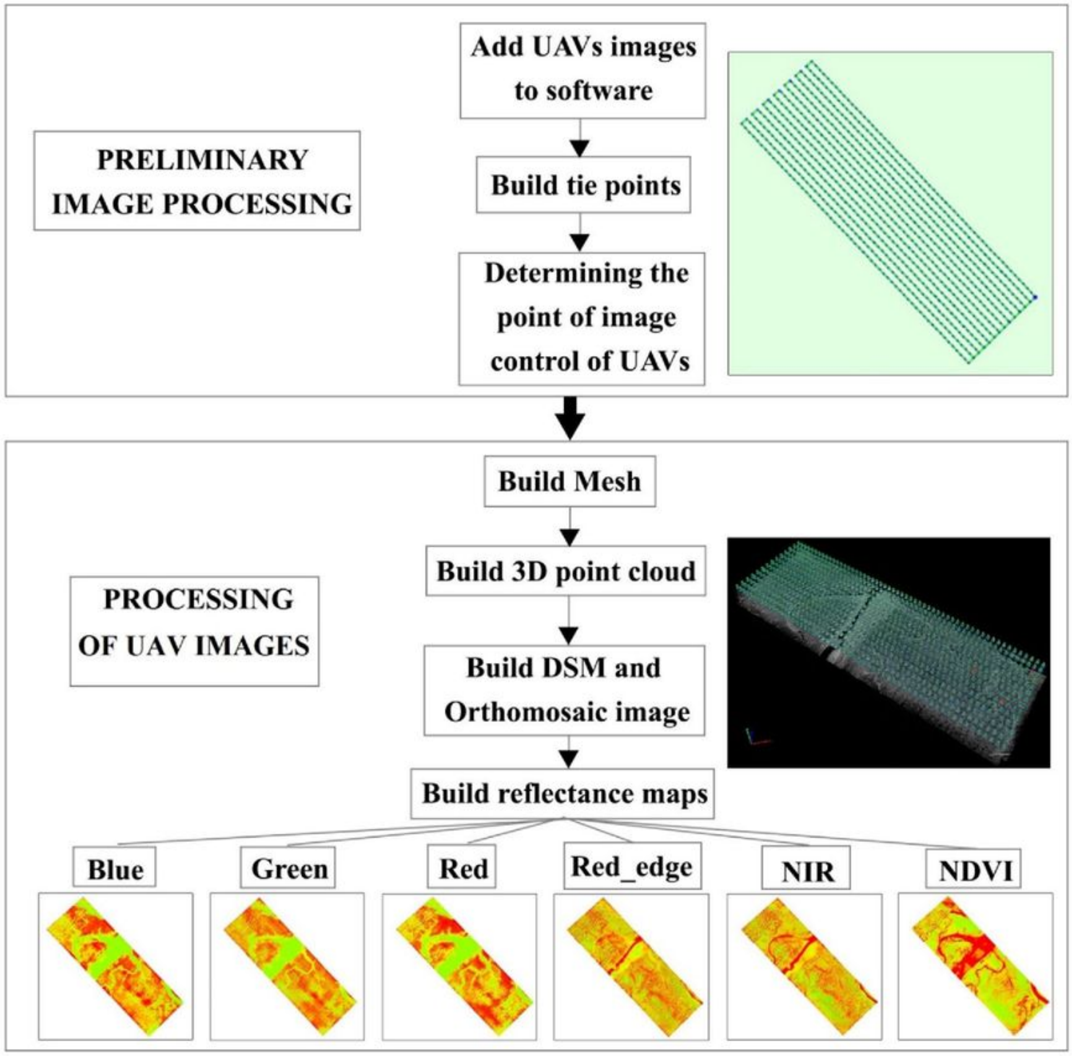

Figure 4

Processing of UAV image using Pix4Dmapper Enterprise 4.4.12 software

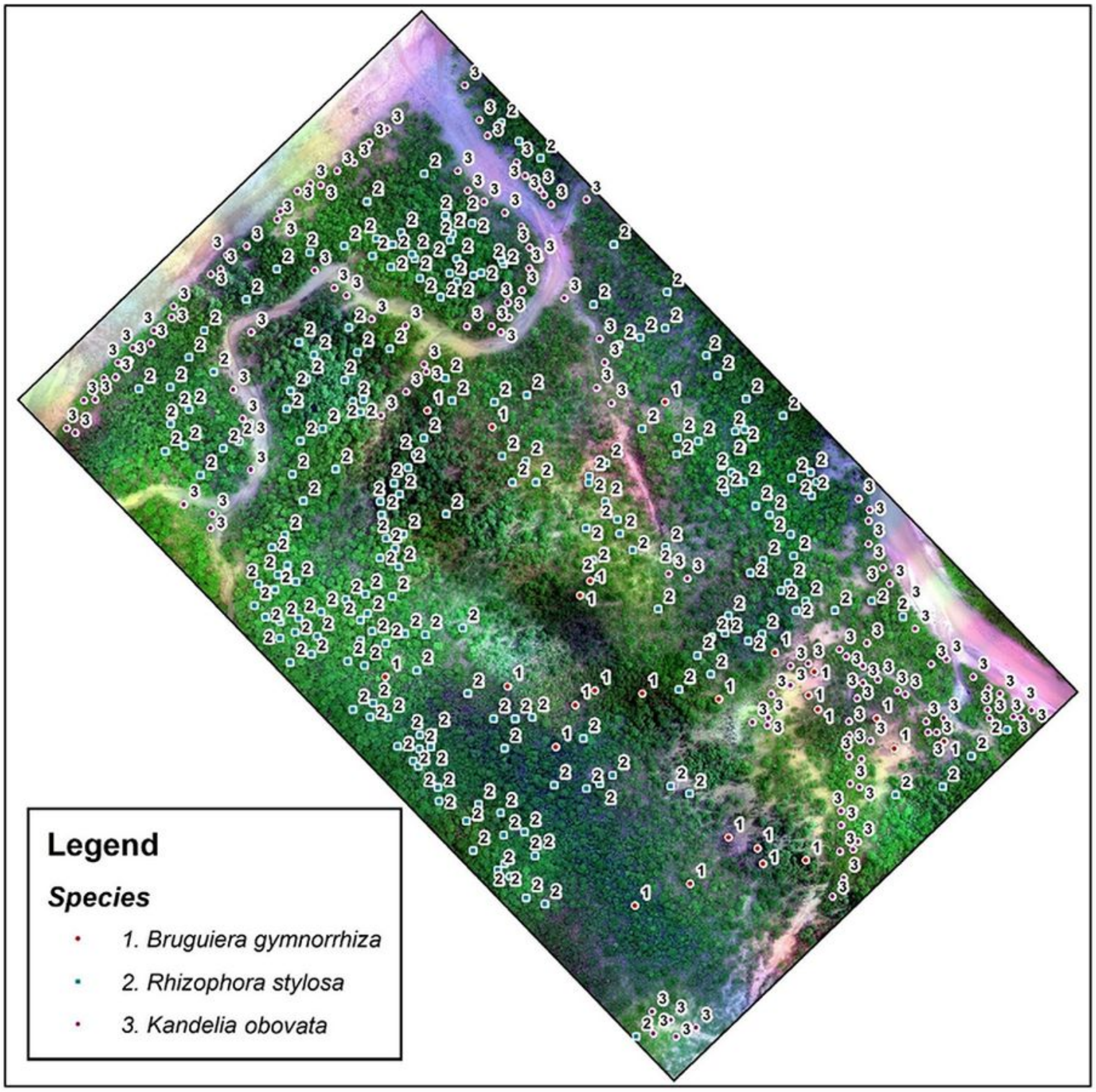

Figure 5

Diagram showing 379 image lock points for accuracy assessment of map in the UAVs-01 area

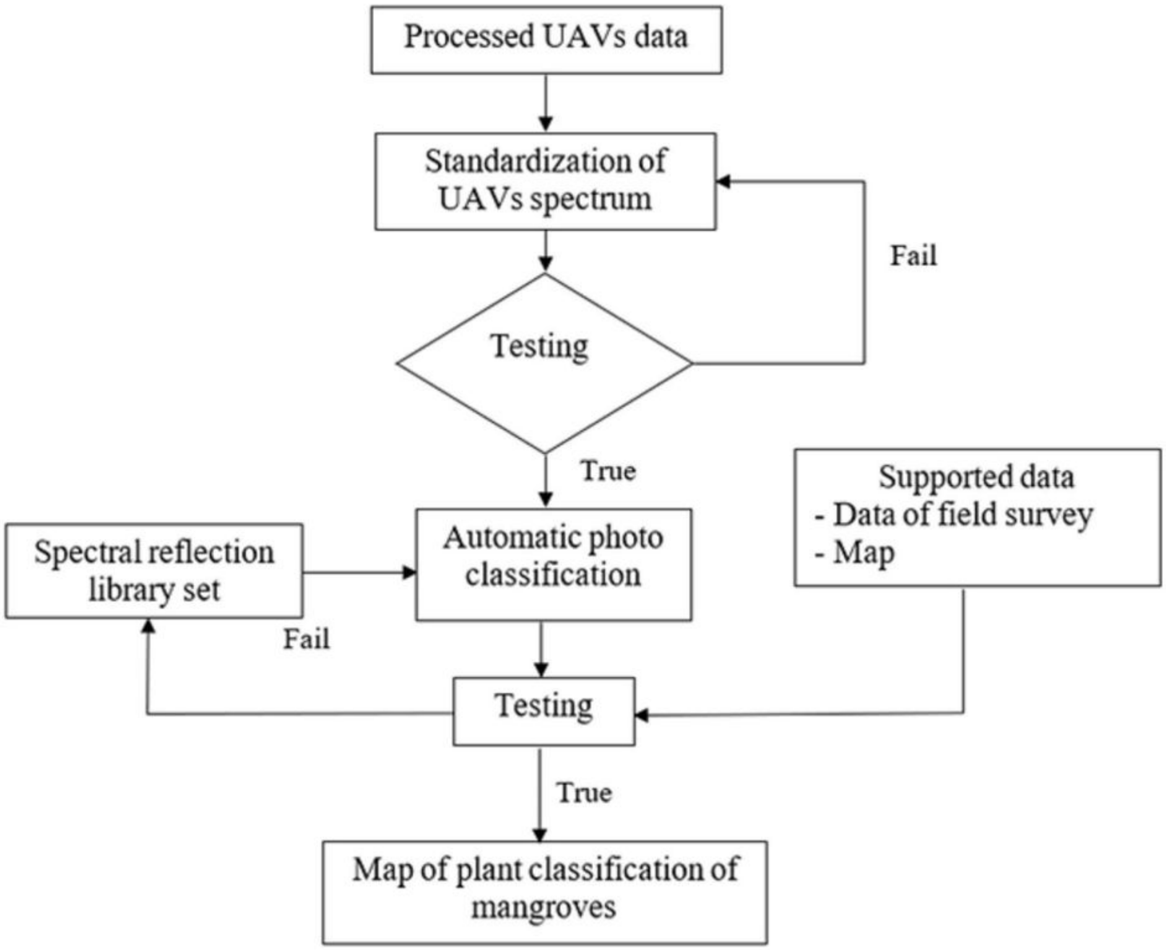

Figure 6

Process for the construction of the tree-species classification map

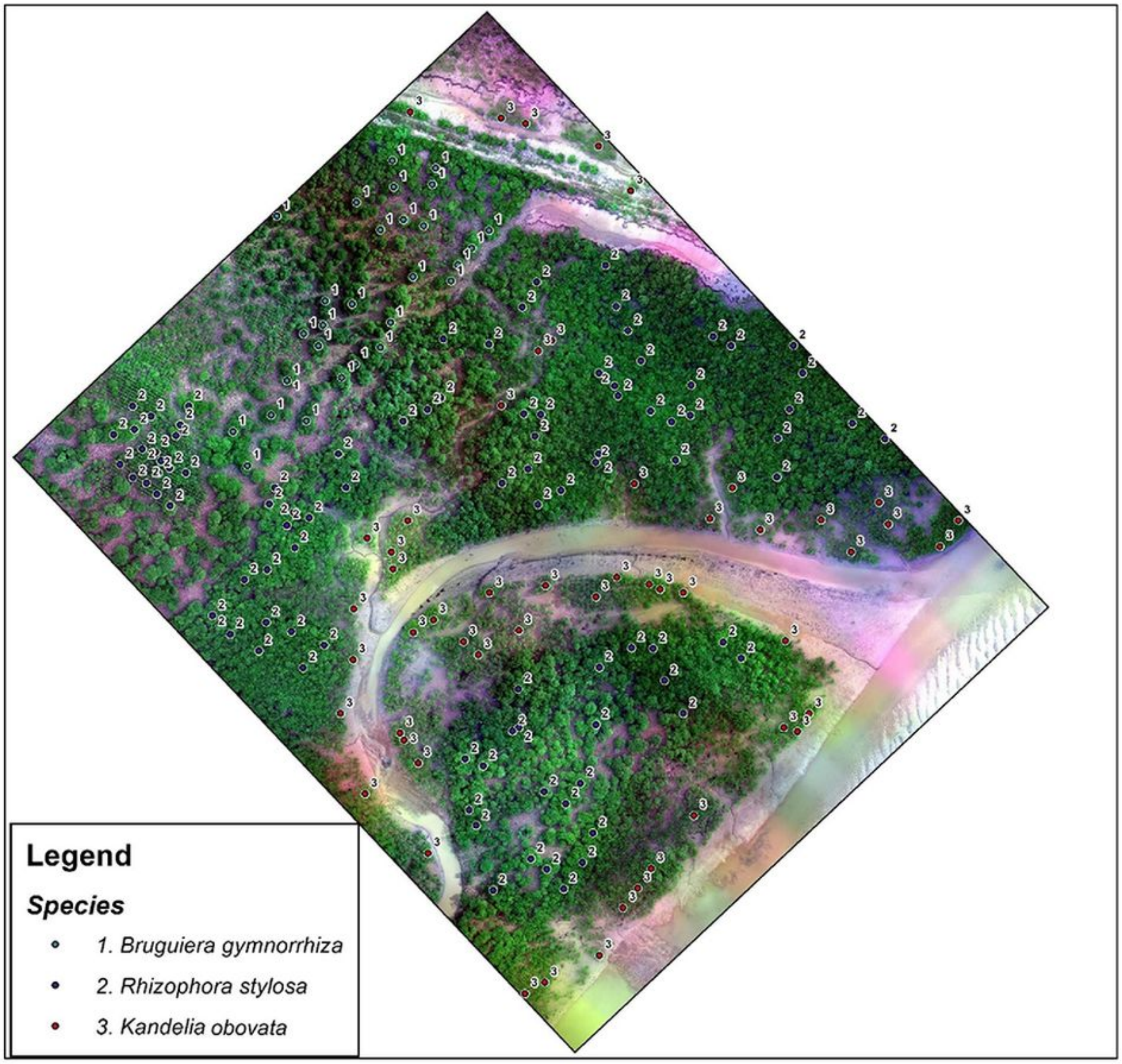

Figure 7

Map showing locations of field survey sites in the UAVs-02 area

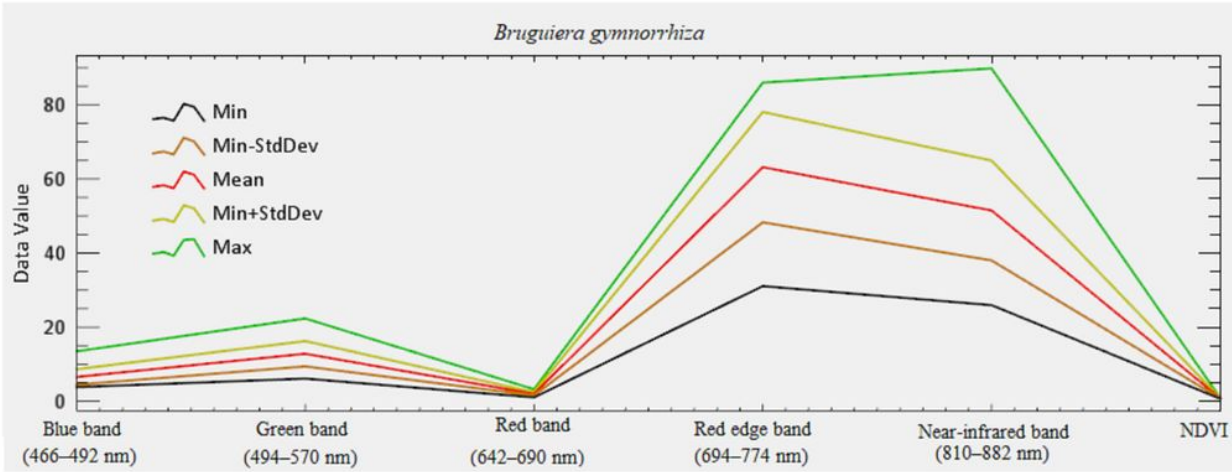

Figure 8

Spectral reflectance and NDVI values of five single-spectral channels for *Bruguiera gymnorrhiza*

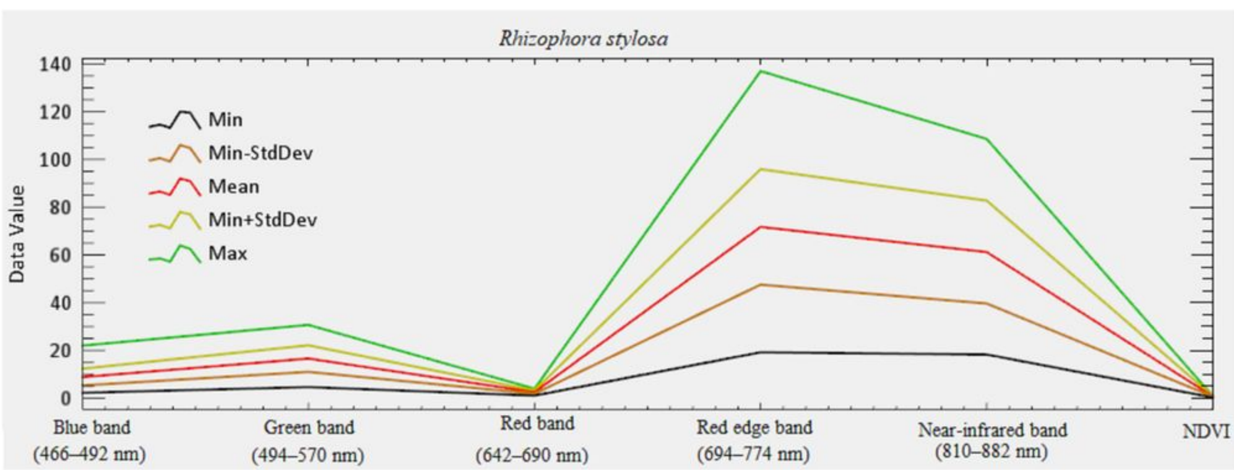

Figure 9

Spectral reflectance and NDVI values of five single-spectral channels for *Rhizophora stylosa*

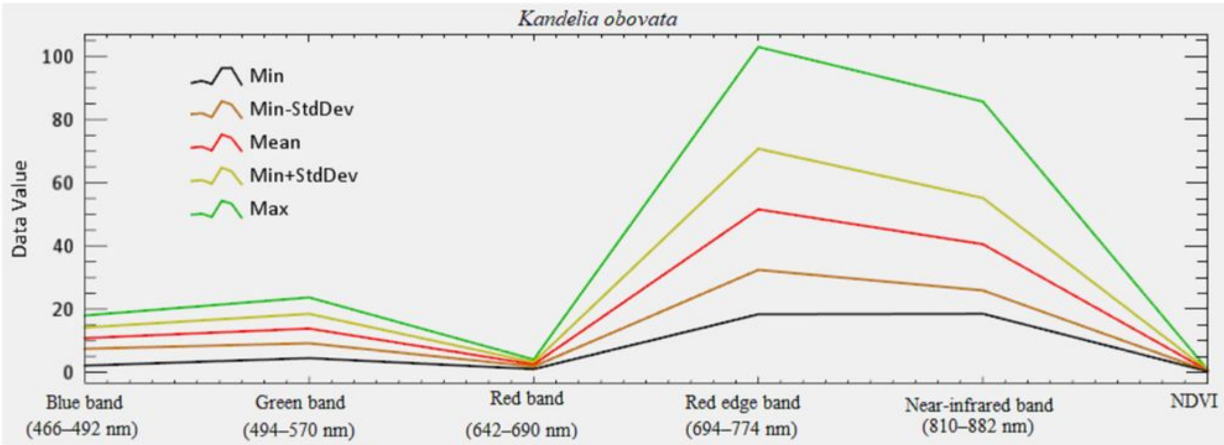

Figure 10

Spectral reflectance and NDVI values of five single-spectral channels for *Kandelia obovata*

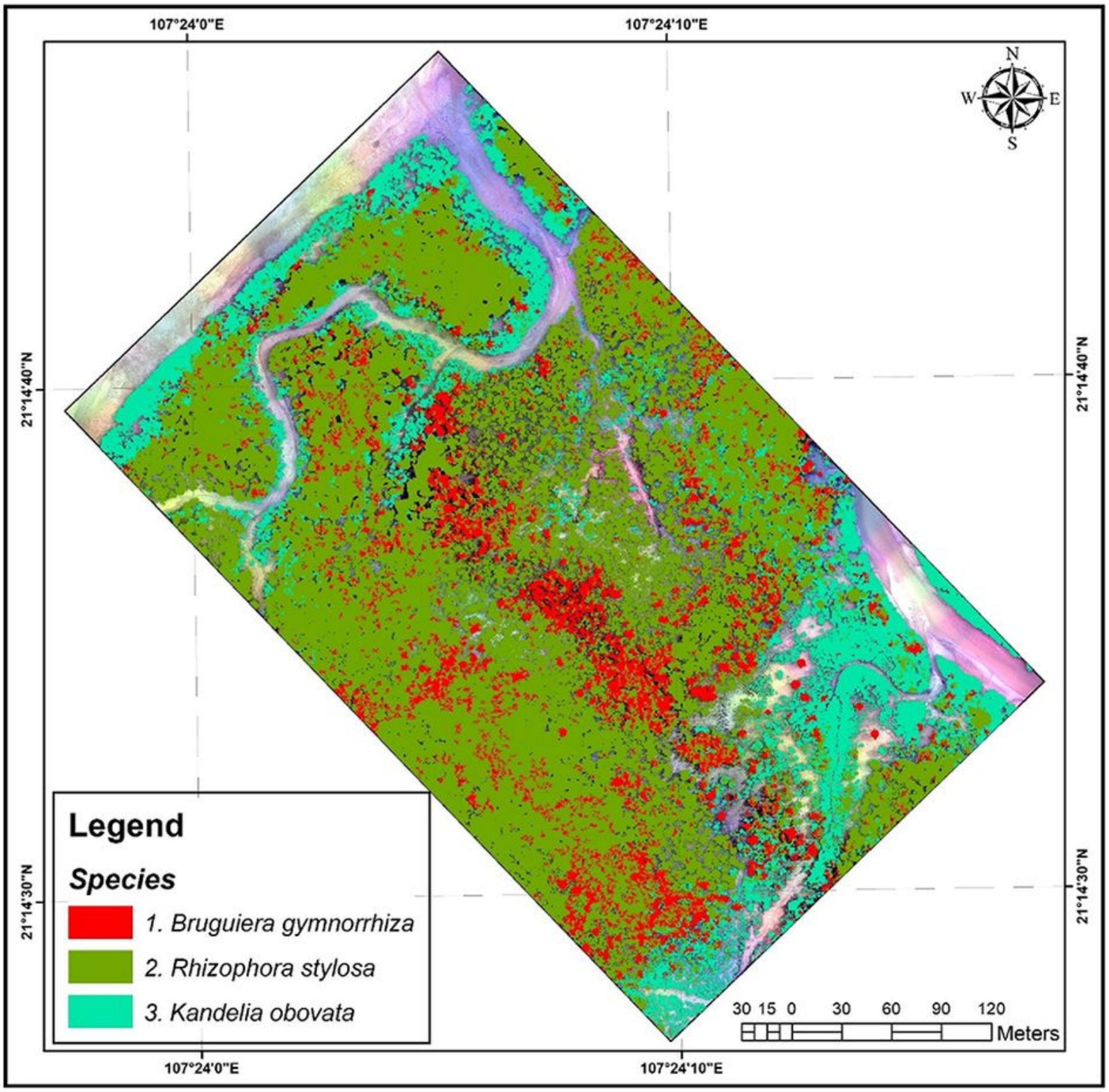

Figure 12

Tree-species classification map of the UAVs-01 area

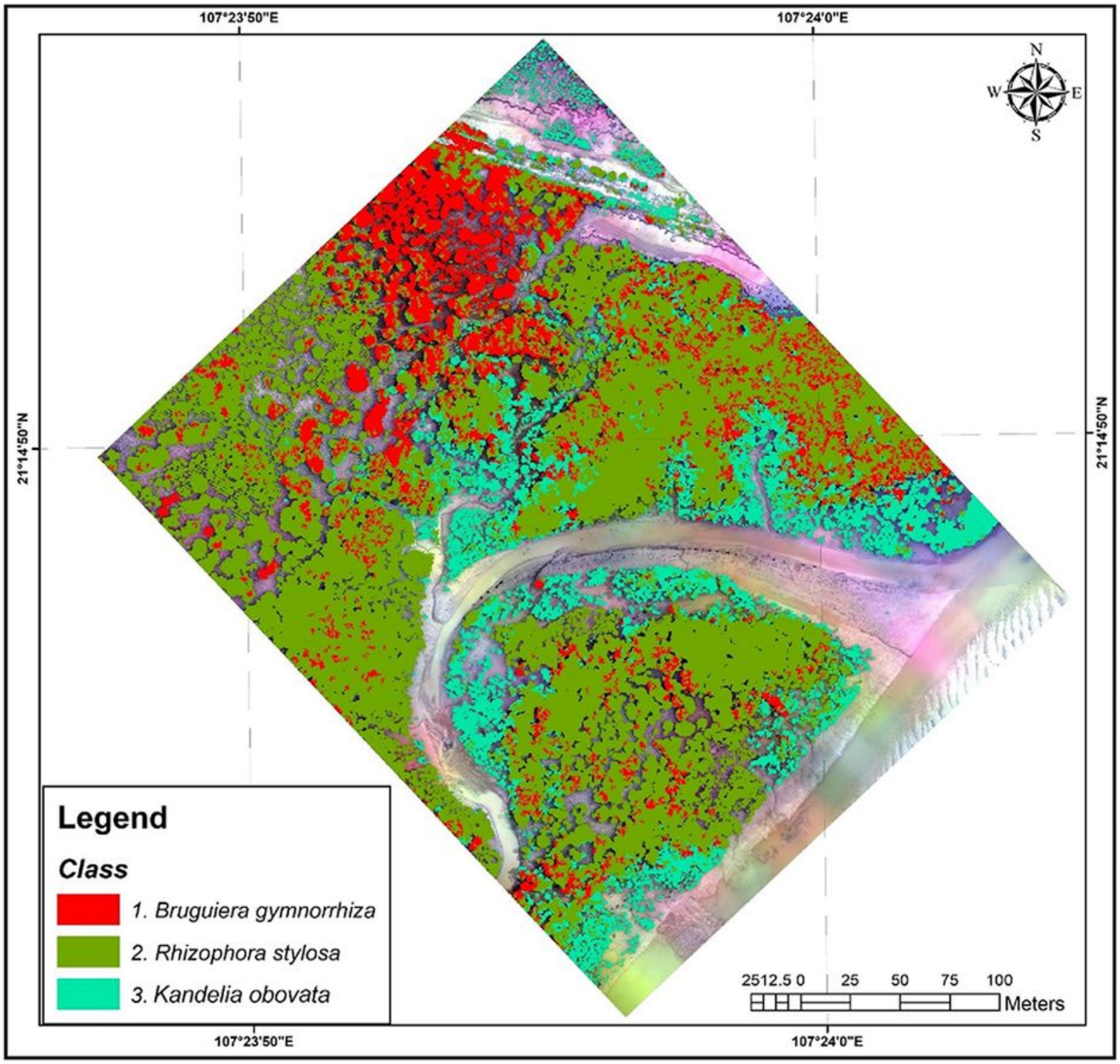

Figure 13

Tree-species classification map of the UAVs-02 area